Adaptive Vision System for Segmentation of Echographic Medical Images based on a Modified Mumford-Shah Functional

Dimitris K. Iakovidis, Michalis A. Savelonas, and Dimitris Maroulis

Dept. of Informatics and Telecommunications, University of Athens,
Panepistimioupolis, 15784, Athens, Greece
dimitris.iakovidis@ieee.org

Abstract. This paper presents a novel adaptive vision system for accurate segmentation of tissue structures in echographic medical images. The proposed vision system incorporates a level-set deformable model based on a modified Mumford-Shah functional, which is estimated over sparse foreground and background regions in the image. This functional is designed so that it copes with the intensity inhomogeneity that characterizes echographic medical images. Moreover, a parameter tuning mechanism has been considered for the adaptation of the deformable model parameters. Experiments were conducted over a range of echographic images displaying abnormal structures of the breast and of the thyroid gland. The results show that the proposed adaptive vision system stands as an efficient, effective and nearly objective tool for the segmentation of echographic images.

1 Introduction

Echographic medical images provide a means for non-invasive in-vivo diagnostics. However, they are inherently characterized by noise, speckle, spatial aliasing and sampling artifacts, causing the boundaries of tissue structures to appear indistinct and disconnected. The shape of these boundaries can be a substantial clue in differential diagnosis, as it is often correlated with malignancy risk [1-2]. A vision system for automatic segmentation of echographic images would be an aid in medical diagnosis, even to experienced radiologists, by providing a nearly objective second opinion based on explicit image features.

A variety of vision systems incorporating different image processing and pattern recognition methods have been proposed for the segmentation of echographic medical images. These include, minimum cross entropy thresholding [3], region growing methods [4-5], classification methods [6], clustering methods [7], wavelet analysis [8], mathematical morphology [9], genetic and fuzzy algorithms [10-11]. State of the art vision systems based on deformable models [12] exhibit advantageous performance in echographic medical image segmentation [13-15]. They are capable of accommodating the complexity and variability of such images by an inherent self-

adapting mechanism that leads to continuous, closed or open, curves without requiring edge-linking operations.

Two-dimensional deformable models involve a contour deformation process which is realized by the minimization of an energy functional designed so that its local minimum is reached at the boundaries of a target object. The energy functional in its basic form comprises of a term that controls the smoothness of the contour and an image dependent term that forces the contour towards the boundaries of the objects. Mumford and Shah [16] formulated an energy functional that contributes to noise resistance by incorporating integrals over image regions. Based on that functional, Chan and Vese [17] developed a level set deformable model that allows the detection of objects whose boundaries are either smooth or not necessarily defined by gradient. The level set approach was introduced to allow for topological changes of the contour during its evolution and it is therefore capable of detecting multiple objects in an image. However, Chan-Vese model assumes that image intensity is piecewise constant, which is hardly true for echographic medical images. This assumption is violated because of single or multiple intensity spikes in such images, attributed to the characteristics of the tissue being examined, to the presence of artifacts such as calcifications, or to external causes such as speckle, usually related to the echographic imaging devices used.

A drawback in the application framework of deformable models to echographic medical image segmentation is that it is device dependent; meaning that for the segmentation of images acquired from different echographic imaging devices, or from the same echographic imaging device using different settings (e.g. dynamic range), a set of different parameter values is required. In most cases parameter tuning requires technical skills and time-consuming manual interaction, which could hardly be performed by radiologists.

In this paper we present a novel vision system for accurate segmentation of echographic images. It incorporates a level-set deformable model based on a modified Mumford-Shah functional estimated over sparse foreground and background regions in the image in order to cope with the presence of inhomogeneity. Moreover, the proposed system utilizes a genetic algorithm to adapt its parameters to the settings of the echographic imaging device used. The performance of the proposed system is evaluated for the segmentation of abnormal structures in breast and thyroid echographic images.

The rest of this paper is organized in three sections. Section 2 describes the proposed system, whereas the results from its application on echographic medical images are apposed in Section 3. Finally, Section 4 summarizes the conclusions of this study and suggests future research perspectives.

2 The Proposed System

The proposed echographic image segmentation system has two modes of operation: adaptation and testing. During the adaptation mode the parameters of the deformable model are tuned so that the system adapts to the settings of the echographic imaging device, based on ground truth information provided by expert radiologists. The test-

ing mode refers to the segmentation of echographic medical images by a tuned deformable model. In what follows we describe the deformable model and the genetic algorithm used.

2.1 Deformable Model based on Modified Mumford-Shah Functional

Mumford-Shah functional is defined as follows [16]:

$$\begin{aligned} F^{MS}(u,C) &= \mu \cdot Length(C) \\ &+ \lambda \int_{\Omega} |u_0(x,y) - u(x,y)|^2 \, dxdy \\ &+ \int_{\Omega / C} |\nabla u(x,y)|^2 \, dxdy \end{aligned} \tag{1}$$

where C is an evolving curve in Ω, where Ω is a bounded open subset of R^2, and μ, λ are positive parameters. The segmentation of an echographic image $u_0 : \Omega \to R$ can be formulated as a minimization problem: We seek for the infimum of the functional $F^{MS}(u,C)$. The solution image $u(x, y)$ obtained by minimizing this functional is formed by smooth regions with sharp boundaries. In the level set method [18], $C \subset \Omega$ is represented by the zero level set of a Lipschitz function $\phi : \Omega \to R$, such that:

$$\begin{aligned} &C = \{(x,y) \in \Omega : \phi(x,y) = 0\}, \\ &inside(C) = \{(x,y) \in \Omega : \phi(x,y) > 0\}, \\ &outside(C) = \{(x,y) \in \Omega : \phi(x,y) < 0\} \end{aligned} \tag{2}$$

Considering that $u(x, y)$ is defined as:

$$u(x,y) = \begin{cases} c^+, & (x,y) \in inside\, C \\ c^-, & (x,y) \in outside\, C \end{cases} \tag{3}$$

Eq. (1) becomes:

$$\begin{aligned} F(c^+, c^-, C) &= \mu \cdot Length(C) \\ &+ \lambda^+ \int_{inside\ C} |u_0(x,y) - c^+|^2 \, dxdy \\ &+ \lambda^- \int_{outside\ C} |u_0(x,y) - c^-|^2 \, dxdy \end{aligned} \tag{4}$$

where c^+ and c^- are average intensities of only a subset of pixels in the foreground (inside C) and in the background (outside C) respectively. This subset is selected so that the pixels contributing most to local inhomogenity are excluded. It is worth noting that the Chan-Vese model considers the average intensities from all the pixels in the respective regions [17]. The values of c^+ and c^- are estimated by the following equations:

$$c^{+}(\phi)=\frac{\int_{\Omega} u_0(x,y)H(\phi(x,y))H(\phi_0(x,y))\Delta_1(x,y)dxdy}{\int_{\Omega} H(\phi(x,y))H(\phi_0(x,y))\Delta_1(x,y)dxdy} \quad (5)$$

$$c^{-}(\phi)=\frac{\int_{\Omega} u_0(x,y)(1-H(\phi(x,y)))H(\phi_0(x,y))\Delta_2(x,y)dxdy}{\int_{\Omega} (1-H(\phi(x,y)))H(\phi_0(x,y))\Delta_2(x,y)dxdy} \quad (6)$$

where H is the Heaviside function. The differences $\Delta_1(x,y)$ and $\Delta_2(x,y)$ are introduced for the cases of foreground and background respectively, as:

$$\Delta_i(x,y)=H(\phi(x,y)+a_i)-H(\phi(x,y)) \quad (7)$$

where i = 1, 2 and α_1,α_2 are constants, negative in the case of the foreground and positive in the case of background. Their value is determined so that $[0,a_1]$ and $[-a_2,0]$ define the acceptable ranges of $\phi(x,y)$ for a point (x,y) to be included in the calculations for the sparse foreground and background region, respectively. Equation (6) implies that the points (x,y) for which $\phi(x,y)$ does not belong in the acceptable range result in $\Delta_i(x,y)\approx 0$. These points correspond to intensity inhomogeneity and cause abrupt changes of ϕ, resulting in $H(\phi(x,y)+a_i)=H(\phi(x,y))$.

Moreover, we assume that the initial contour as traced by ϕ_0 corresponds to the region of interest and we employ $H(\phi_0)$ to restrict the calculation of the average foreground and background intensities c^{+} and c^{-} over this region.

Keeping c^{+} and c^{-} fixed, and minimizing F with respect to ϕ, the associated Euler-Langrange equation for ϕ is deduced. Finally, ϕ is determined by parameterizing the descent direction by an artificial time $t\geq 0$, and solving the following equation

$$\frac{\partial\phi}{\partial t}=\delta(\phi)[\mu\cdot div(\frac{\nabla\phi}{|\nabla\phi|})-\lambda^{+}(u_0-c^{+})^2+\lambda^{-}(u_0-c^{-})^2]=0 \quad (8)$$

where $t\in(0,\infty),(x,y)\in\Omega$ and δ is the one-dimensional Dirac function.

2.2 Genetic Algorithm

The genetic algorithm used in the adaptation mode aims at parameter tuning of the deformable model. Genetic algorithms are stochastic non-linear optimization algorithms based on the theory of natural selection and evolution [19-20]. They have been the optimizers of choice in various artificial intelligence applications, exhibiting better performance than other non-linear optimization approaches to parameter tuning [21-24].

Motivated by these studies, we transcribed the parameter tuning optimization problem of the level-set deformable model into a genetic optimization problem. Considering that μ, λ^{+}, λ^{-} are weight terms of the energy functional that regulate the

relative influence of the terms comprising Eq. (1), and that $\mu > 0$, (6) can be rewritten as follows:

$$\delta(\phi)[div(\frac{\nabla\phi}{|\nabla\phi|}) - \frac{\lambda^+}{\mu}(u_0 - c^+)^2 + \frac{\lambda^-}{\mu}(u_0 - c^-)^2] = 0 \quad \textbf{(9)}$$

and by setting $k^+ = \frac{\lambda^+}{\mu}$ and $k^- = \frac{\lambda^-}{\mu}$, (7) can be rewritten as follows:

$$\delta(\phi)[div(\frac{\nabla\phi}{|\nabla\phi|}) - k^+(u_0 - c^+)^2 + k^-(u_0 - c^-)^2] = 0 \quad \textbf{(10)}$$

The parameters k^+, k^-, α_1 and α_2 are encoded into a single bit-string, called chromosome. Their values are constrained within discrete, worst-case ranges determined experimentally. Two 6-bit variables with integer values ranging from 0 to 64, are used to hold k^+ and k^+, and two 4-bit variables are used to hold the exponents of α_1 and α_2, enumerating the values $10^{-15}, 10^{-14}, ..., 10^0$. The length l of the resulting chromosome sums a total of 20-bits.

In the adaptation mode the genetic algorithm searches for the chromosome associated with the optimal parameters (k, α_1 and α_2) which maximize the overlap value f between a contour A and a given ground truth segmentation T of the target tissue structure. The ground truth segmentation comprises of all pixels falling within at least $N/2+1$ segmentations out of N segmentations drawn by N radiologists [25]. The bias introduced in the ground truth segmentation is reduced as N increases. The overlap value f between two delineated areas A and T is defined as in [5]:

$$f = \frac{A \cap T}{A \cup T}. \quad \textbf{(11)}$$

In case of a perfect match between the two delineated areas A and T, the overlap value is maximized ($f = 1$).

The genetic algorithm of the adaptation mode proceeds to the reproduction of an initial population of R chromosomes by following the steady state approach [26]. The fittest individuals are maintained in the population and they are used to generate offspring individuals by multi-parent diagonal crossover [27]. Following crossover, a mutation operator is applied, flipping the bit content of the chromosomes at random positions from 1 to 0, and vice versa, with very low probability [28]. This operation provides a mechanism to keep the solution away from local minima [24].

The genetic algorithm can be summarized in pseudocode as follows (where G is the current generation):

Step 1. Initialize $G \leftarrow 0$, $f_{\text{FITTEST}} \leftarrow 0$
Generate Population of R Chromosomes at random
Step 2. For each Chromosome
Execute deformable model on input image
Calculate $f(G)$
If $f(G) \geq f_{\text{FITTEST}}$ Then

$f_{\text{FITTEST}} \leftarrow f(G)$
Register f_{FITTEST}
End If
End For

Step 3. $G \leftarrow G + 1$

Step 4. Begin Reproduction
Select Fittest Chromosomes
Maintain Fittest Chromosomes in the Population
End Reproduction

Step 5. Crossover Fittest Chromosomes to Generate new Chromosomes

Step 6. Mutate Fittest Chromosomes to Generate new Chromosomes

Step 7. Repeat Steps 2 to 6 Until $G = G_{\max}$

The parameter tuning procedure, described above, will result in a registered optimal set of parameters (k, α_1 and α_2). This set of parameters can be used for the segmentation of similar tissue structures in other medical images acquired from the same imaging device with the same settings.

3 Results

Experiments were performed aiming at the assessment of the proposed vision system for the segmentation of echographic medical images. The dataset used in the experiments comprised of 38 breast and thyroid echographic images (Table 1), containing abnormal tissue structures. The images were digitized at 256×256-pixel dimensions and at 8-bit grey level depth.

The proposed vision system was implemented in Microsoft Visual C++ and executed on a 3.2 GHz Intel Pentium IV workstation. The parameters of the genetic algorithm were kept constant during the experimentation. A typical population of $R = 30$ chromosomes was considered in agreement with [29]. The crossover probability was set at 0.6 [30] and the mutation probability was set at $1/l = 0.05$, where the length of the chromosome was $l = 20$ [31]. A number of $G_{max} = 50$ generations was considered, as it allows for convergence to the highest attainable fitness value.

The adaptation mode accepts a single echographic image for parameter tuning. In order to avoid the sample selection bias that would be introduced if the performance evaluation process used a single image for parameter tuning, arbitrarily selected from the available set of images, a cross-validation scheme was employed [32]. This scheme involved multiple experiments that use independent images for parameter tuning and testing. In each experiment, a different image was drawn from the dataset and used for parameter tuning, whereas the rest of the dataset was used for testing.

The average overlaps obtained by the proposed vision system and the individual radiologists are summarized in Table 1. These results provide an estimate of the generalization ability of the system. The obtained segmentation accuracies are comparable to or even higher than the segmentation accuracies obtained by individual radiologists. The latter case can be attributed to the subjectivity induced in the segmenta-

tions obtained by individual radiologists, which is associated with interobserver variability.

Table 1. Average segmentation accuracy with respect to the ground truth, for the individual radiologists and the proposed system.

Subject	**Images**	**Radiologists *v* (%)**	**Proposed System *v* (%)**
Breast findings	20	89.1±1.7	92.7±1.1
Thyroid findings	18	90.7±2.3	94.4±1.7

The interobserver variability as quantified by the coefficient of variation [33] ranges between 2.1% and 11.8%. The coefficient of variation of the overlap values obtained with the proposed vision system ranges between 0.9% and 3.0%, and in all the cases, it was lower than the coefficient of variation of the radiologists.

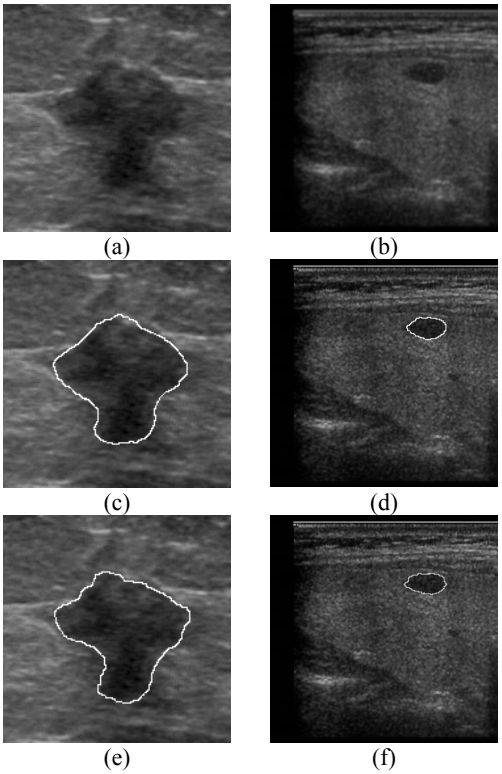

Fig. 1. Echographic medical images and segmentation results, (a) echographic image of a breast nodule, (b) echographic image of a thyroid nodule, (c-d) segmentations obtained by individual expert radiologists, (e-f) segmentations obtained by the proposed segmentation approach.

Figure 1 illustrates two indicative echographic medical images used in the experiments. The first image (Fig. 1a) illustrates an echographic image of a breast nodule. The overlap obtained with the proposed vision system is 94.5% (Fig. 1c), whereas the overlap obtained by an individual radiologist is 92.1% (Fig. 1e) respectively. The second image (Fig. 1b) illustrates an echographic image of a thyroid nodule. The overlap obtained with the proposed vision system is 98.9% (Fig. 1d) whereas the overlap achieved by an individual radiologist is slightly higher reaching 97.0% (Fig. 1f).

The average time required for the execution of the segmentation algorithm is of the order of a minute. The maximum time required in the adaptation mode of the proposed vision system reaches approximately the 18h, but it needs to run only once for a particular imaging device. It should be noted that if one had to follow the naive approach of exhaustive search in the parameter space, the execution time required would be up to three orders of magnitude higher. The resulting set of optimal parameters (k^+, k^+, α_1 and α_2) may be applied for the segmentation of abnormal tissue structures in other similar echographic images acquired from the same echographic imaging device with the same settings. This means that for each new image, only the execution time of the deformable model is required.

4 Conclusion

We have introduced a novel vision system, which embodies a level-set deformable model tuned by a genetic algorithm. The deformable model is based on a modified Mumford-Shah functional, which is estimated over sparse foreground and background regions in the image, so as to cope with the intensity inhomogeneity characterizing echographic medical images. The genetic algorithm has been employed for efficient tuning of the parameters of the deformable model to an optimal set of values for the particular settings of the imaging device used. This adaptation of the deformable model allows accurate segmentations of tissue structures in echographic medical images. The segmentation accuracy provided is comparable to or even higher than the segmentation accuracies obtained by individual radiologists.

The results show that the interobserver variability of the individual radiologists is higher than the variability of the overlap values obtained with the proposed vision system. Therefore, this vision system offers a tool for nearly objective clinical assessment of tissue structures. Moreover, it provides the radiologists with a second opinion, without requiring technical skills or time-consuming manual interaction for parameter tuning.

Future research perspectives include speed up of the proposed system, and its embedment into an integrated system that will combine heterogeneous information to support diagnosis.

Acknowledgement

We would like to thank Dr. N. Dimitropoulos M.D. Radiologist, and EUROMEDICA S.A., Greece, for the provision of the echographic images and their contribution in the evaluation of the results. This work was supported by the Greek General Secretariat of Research and Technology and the European Social Fund, through the PENED 2003 program (grant no. 03-ED-662).

References

1. Ching H.K. et al: Stepwise Logistic Regression Analysis of Tumor Contour Features for Breast Ultrasound Diagnosis. Proc IEEE Ultr Symp, Vol. 2, Atlanta, GA, USA (2001)1303-1306
2. Papini E. et al: Risk of Malignancy in Nonpalpable Thyroid Nodules: Predictive Value of Ultrasound and Color-Doppler Features. J Clin Endocrin & Metabol, Vol. 87, No. 5 (2002) 1941-1946
3. Zimmer Y., Tepper R., Akselrod S.: A two-dimensional extension of minimum cross entropy thresholding for the segmentation of ultrasound images. Ultr Med and Biol, Vol. 22, (1996) 1183-1190
4. Adams R., Bischof L.: Seeded region growing. IEEE Trans Pat Anal Mach Intel, Vol. 16, No.6, (1994) 641-647
5. Hao X., Bruce C., Pislaru C., Greenleaf J.F.: A Novel Region Growing Method for Segmenting Ultrasound Images. Proc IEEE Int Ultr Symp, Vol. 2 (2000) 1717-1720
6. Kotropoulos C., Pittas I.: Segmentations of Ultrasonic Images Using Support Vector Machines. Pat Rec Let, Vol. 24, Elsevier Science (2003) 715-727
7. Boukerroui D., Basset O., Guerin N., Baskurt A.: Multiresolution Texture Based Adaptive Clustering Algorithm for Breast Lesion Segmentation. Eur. J Ultr, Vol. 8 (1998) 135-144
8. Fan L., Braden G.A., Herrington D.M.: Nonlinear Wavelet Filter for Intracoronary Ultrasound Images. Proc An Meet Comp Card (1996) 41-44
9. Thomas J.G., Peters R.A., Jeanty P.: Automatic Segmentation of Ultrasound Images Using Morphological Operators. IEEE Trans Med Im, Vol. 10 (1991) 180-186
10. Heckman T.: Searching for Contours. Proc SPIE, Vol. 2666 (1996) 223-232
11. Solaiman B., Roux C., Rangayyan R.M., Pipelier F., Hillion A.: Fuzzy Edge Evaluation in Ultrasound Endosonographic Images. Proc Can Conf Elec Comp Eng (1996) 335-338
12. McInerney T., Terzopoulos D.: Deformable Models in Medical Image Analysis: A Survey. Med Im Anal, Vol. 1, No. 2 (1996) 91-108
13. Honggang Y., Pattichis M.S., Goens M.B.: Robust Segmentation of Freehand Ultrasound Image Slices Using Gradient Vector Flow Fast Geometric Active Contours, Proc IEEE South Symp Im Anal Interpr (2006) 115-119
14. Liu W., Zagzebski J.A., Varghese T., Dyer C.R., Techavipoo U., Hall T.J.: Segmentation of Elastographic Images Using a Coarse-to-Fine Active Contour Model. Ultr Med Biol, Vol. 32, No. 3 (2006) 397-408
15. Cardinal M.-H.R., Meunier J., Soulez G., Maurice R.L., Therasse E., Cloutier G.: Intravascular Ultrasound Image Segmentation: a Three-Dimensional Fast-Marching Method Based on Gray Level Distributions. IEEE Trans Med Im, Vol. 25, No. 5 (2006) 590-601
16. Mumford D., Shah J.: Optimal Approximation by Piecewise Smooth Functions and Associated Variational Problems. Commun Pure Appl Math, Vol. 42 (1989) 577-685

17. Chan T.F., Vese L.A.: Active Contours Without Edges, IEEE Trans Im Proc, Vol. 7 (2001) 266-277
18. Osher S., Sethian J.: Fronts Propagating with Curvature-Dependent Speed: Algorithms Based on the Hamilton-Jacobi Formulations. J Comp Phys, Vol. 79 (1988) 12-49
19. Goldberg D.E.: Genetic Algorithms in Search, Optimization and Machine Learning. Addison-Wesley: Reading, MA (1989)
20. Grefenstette J.J.: Optimization of Control Parameters for Genetic Algorithms. IEEE Trans Syst Man Cyber, Vol. 16, No. 1 (1986) 122–128
21. Min S.H., Lee J., Han I.: Hybrid Genetic Algorithms and Support Vector Machines for Bankruptcy Prediction. Expert Systems with Applications, Vol. 31, No. 3, Elsevier Science, (2006) 652-660
22. Zhao X.M., Cheung Y.M., Huang D.S.: A Novel Approach to Extracting Features from Motif Content and Protein Composition for Protein Sequence Classification. Neural Networks, Vol. 18, Elsevier Science (2005) 1019-1028
23. Plagianakos V.P, Magoulas G.D., Vrahatis M.N.: Tumor Detection in Colonoscopic Images Using Hybrid Methods for On-Line Neural Network Training. Proc Int Conf Neur Net Exp Syst Med Health (2001) 59-64
24. Pignalberi G., Cucchiara R., Cinque L., Levialdi S.: Tuning Range Segmentation by Genetic Algorithm. EURASIP J Appl Sig Proc, Vol. 8 (2003) 780-790
25. Kaus M.R., Warfield S.K., Jolesz F.A., Kikinis R.: Segmentation of Meningiomas and Low Grade Gliomas in MRI.: Proc Int Conf Med Im Comp Comp-Ass Interv (1999) 1-10
26. Syswerda G.: A Study of Reproduction in Generational and Steady State Genetic Algorithms.: Foundations of Genetic Algorithms, Rawlings G.J.E., San Mateo: Morgan Kaufmann (1999) 94-101
27. Eiben A.E.: Multiparent Recombination in Evolutionary Computing, Advances in Evolutionary Computing.: Natural Computing Series, Springer Verlag, Berlin Heidelberg New York (2002) 175-192
28. Bäck T.: Optimal Mutation Rates in Genetic Search.: Proc Int Conf Gen Alg (1993) 2-8
29. Goldberg D.E.: Sizing Population for Serial and Parallel Genetic Algorithms. Proc Int Conf Gen Alg (1989) 70-79
30. Bäck T., Hammel U., Schwefel H.P.: Evolutionary Computation: Comments on the History and Current State. IEEE Trans Evol Comp, Vol. 1, No. 1 (1997) 3-17
31. Kemenade K.M. van, Eiben A.E.: Multi-Parent Recombination to Overcome Premature Convergence in Genetic Algorithms. Proc Dutch Conf Art Intell (1995) 137-146
32. Theodoridis S., Koutroumbas K.: Pattern Recognition. Academic Press (1998)
33. Woltjer H.H.: The Intra- and Interobserver Variability of Impedance Cardiography in Patients at Rest During Exercise. Physiol Meas, Vol. 17 (1996) 171-178